TIRF images were taken with an Olympus IX81 microscope equipped with a 60 ×, 1.45 numerical aperture objective and a Hamamatsu C4880 CCD camera. For immunofluorescence staining, NBT-II cells stably expressing EGFP–paxillin-β or EGFP–Pax_{S178A} were plated on collagen-coated plastic rectangles (25 mm × 50 mm, cut from the bottom of Petri dishes) and cultured for 12 h. F-actin was stained with Alexa 488 phalloidin, and vinculin was stained with anti-vinculin monoclonal antibody (Sigma), followed by tetramethylrhodamine β-isothiocyanate-labelled anti-mouse antibody. The plastic rectangles were then covered with coverslips. F-actin and vinculin images were observed as described above.

Received 15 April 2002; accepted 13 May 2003; doi:10.1038/nature01745.

1. Ip, Y. T. & Davis, R. J. Signal transduction by the c-Jun N-terminal kinase (JNK)—from inflammation to development. *Curr. Opin. Cell Biol.* **10,** 205–219 (1998).
2. Barr, R. K. & Bogoyevitch, M. A. The c-Jun N-terminal protein kinase family of mitogen-activated protein kinases (JNK MAPKs). *Int. J. Biochem. Cell Biol.* **33,** 1047–1063 (2001).
3. Riesgo-Escovar, J. R., Jenni, M., Fritz, A. & Hafen, E. The *Drosophila* Jun-N-terminal kinase is required for cell morphogenesis but not for DJun-dependent cell fate specification in the eye. *Genes Dev.* **10,** 2759–2768 (1996).
4. Sluss, H. K., Han, Z., Barrett, T., Davis, R. J. & Ip, Y. T. A JNK signal transduction pathway that mediates morphogenesis and an immune response in *Drosophila*. *Genes Dev.* **10,** 2745–2758 (1996).
5. Xia, Y. *et al.* MEK kinase 1 is critically required for c-Jun N-terminal kinase activation by proinflammatory stimuli and growth factor-induced cell migration. *Proc. Natl Acad. Sci. USA* **97,** 5243–5248 (2000).
6. Yujiri, T. *et al.* MEK kinase 1 gene disruption alters cell migration and c-Jun NH_2-terminal kinase regulation but does not cause a measurable defect in NF-κB activation. *Proc. Natl Acad. Sci. USA* **97,** 7272–7277 (2000).
7. Ozanne, B. W. *et al.* Transcriptional regulation of cell invasion: AP-1 regulation of a multigenic invasion programme. *Eur. J. Cancer* **36,** 1640–1648 (2000).
8. Almeida, E. A. *et al.* Matrix survival signaling: From fibronectin via focal adhesion kinase to c-Jun NH_2-terminal kinase. *J. Cell Biol.* **149,** 741–754 (2000).
9. Liu, S. *et al.* Binding of paxillin to α4 integrins modifies integrin-dependent biological responses. *Nature* **402,** 676–681 (1999).
10. Hagel, M. *et al.* The adaptor protein paxillin is essential for normal development in the mouse and is a critical transducer of fibronectin signaling. *Mol. Cell. Biol.* **22,** 901–915 (2002).
11. Schaller, M. D. Paxillin: A focal adhesion-associated adaptor protein. *Oncogene* **20,** 6459–6472 (2001).
12. Bellis, S. L., Perrotta, J. A., Curtis, M. S. & Turner, C. E. Adhesion of fibroblasts to fibronectin stimulates both serine and tyrosine phosphorylation of paxillin. *Biochem. J.* **325,** 375–381 (1997).
13. Vadlamudi, R., Adam, L., Talukder, A., Mendelsohn, J. & Kumar, R. Serine phosphorylation of paxillin by heregulin-β1: role of p38 mitogen activated protein kinase. *Oncogene* **18,** 7253–7264 (1999).
14. Brown, M. C., Perrotta, J. A. & Turner, C. E. Serine and threonine phosphorylation of the paxillin LIM domains regulates paxillin focal adhesion localization and cell adhesion to fibronectin. *Mol. Biol. Cell.* **9,** 1803–1816 (1998).
15. Beningo, K. A., Dembo, M., Kaverina, I., Small, J. V. & Wang, Y. L. Nascent focal adhesions are responsible for the generation of strong propulsive forces in migrating fibroblasts. *J. Cell Biol.* **153,** 881–888 (2001).
16. Lee, J. & Jacobson, K. The composition and dynamics of cell–substratum adhesions in locomoting fish keratocytes. *J. Cell Sci.* **110,** 2833–2844 (1997).
17. Abassi, Y. A. & Vuori, K. Tyrosine 221 in Crk regulates adhesion-dependent membrane localization of Crk and Rac and activation of Rac signaling. *EMBO J.* **21,** 4571–4582 (2002).
18. Hauck, C. R. *et al.* Inhibition of focal adhesion kinase expression or activity disrupts epidermal growth factor-stimulated signaling promoting the migration of invasive human carcinoma cells. *Cancer Res.* **61,** 7079–7090 (2001).
19. Huynh-Do, U. *et al.* Ephrin-B1 transduces signals to activate integrin-mediated migration, attachment and angiogenesis. *J. Cell Sci.* **115,** 3073–3081 (2002).
20. Ridley, A. J., Allen, W. E., Peppelenbosch, M. & Jones, G. E. Rho family proteins and cell migration. *Biochem. Soc. Symp.* **65,** 111–123 (1999).
21. Minden, A., Lin, A., Claret, F. X., Abo, A. & Karin, M. Selective activation of the JNK signaling cascade and c-Jun transcriptional activity by the small GTPases Rac and Cdc42Hs. *Cell* **81,** 1147–1157 (1995).
22. Christerson, L. B., Vanderbilt, C. A. & Cobb, M. H. MEKK1 interacts with alpha-actinin and localizes to stress fibers and focal adhesions. *Cell Motil. Cytoskel.* **43,** 186–198 (1999).
23. Fanger, G. R., Johnson, N. L. & Johnson, G. L. MEK kinases are regulated by EGF and selectively interact with Rac/Cdc42. *EMBO J.* **16,** 4961–4972 (1997).
24. Ilic, D. *et al.* Reduced cell motility and enhanced focal adhesion contact formation in cells from FAK-deficient mice. *Nature* **377,** 539–544 (1995).
25. Oktay, M., Wary, K. K., Dans, M., Birge, R. B. & Giancotti, F. G. Integrin-mediated activation of focal adhesion kinase is required for signaling to Jun NH_2-terminal kinase and progression through the G1 phase of the cell cycle. *J. Cell Biol.* **145,** 1461–1469 (1999).
26. Liu, J., Huang, C. & Zhan, X. Src is required for cell migration and shape changes induced by fibroblast growth factor 1. *Oncogene* **18,** 6700–6706 (1999).
27. Nagata, K. *et al.* The MAP kinase kinase kinase MLK2 co-localizes with activated JNK along microtubules and associates with kinesin superfamily motor KIF3. *EMBO J.* **17,** 149–158 (1998).
28. Small, J. V. & Kaverina, I. Microtubules meet substrate adhesions to arrange cell polarity. *Curr. Opin. Cell. Biol.* **15,** 40–47 (2003).
29. Lee, J., Ishihara, A., Oxford, G., Johnson, B. & Jacobson, K. Regulation of cell movement is mediated by stretch-activated calcium channels. *Nature* **400,** 382–386 (1999).
30. Huang, C., Liu, J., Haudenschild, C. C. & Zhan, X. The role of tyrosine phosphorylation of cortactin in the locomotion of endothelial cells. *J. Biol. Chem.* **273,** 25770–25776 (1998).

Supplementary Information accompanies the paper on **www.nature.com/nature**.

Acknowledgements We thank C. Raska, J. Han and R. M. Pope for their mass spectometric analysis, and K. Burridge, L. Graves and C. Otey for critically reading the manuscript. This study was supported by NIH grants to K.J. and M.D.S., the Cell Migration Consortium to K.J. and the National Institute for Dental and Cranial Research grant to K.J. and M.D.S.

Competing interests statement The authors declare that they have no competing financial interests.

Correspondence and requests for materials should be addressed to K.J. (frap@med.unc.edu)

Acute mutation of retinoblastoma gene function is sufficient for cell cycle re-entry

Julien Sage*, Abigail L. Miller*, Pedro A. Pérez-Mancera‡, Julianne M. Wysocki* & Tyler Jacks*†

** Department of Biology and Centre for Cancer Research, and † Howard Hughes Medical Institute, Massachusetts Institute of Technology, Cambridge, Massachusetts 02139, USA*
‡ Instituto de Biologia Molecular y Celular del Cancer, CSIC/Universidad de Salamanca, 37007-Salamanca, Spain

Cancer cells arise from normal cells through the acquisition of a series of mutations in oncogenes and tumour suppressor genes[1]. Mouse models of human cancer often rely on germline alterations that activate or inactivate genes of interest. One limitation of this approach is that germline mutations might have effects other than somatic mutations, owing to developmental compensation[2,3]. To model sporadic cancers associated with inactivation of the retinoblastoma (*RB*) tumour suppressor gene in humans, we have produced a conditional allele of the mouse *Rb* gene. We show here that acute loss of *Rb* in primary quiescent cells is sufficient for cell cycle entry and has phenotypic consequences different from germline loss of *Rb* function. This difference is explained in part by functional compensation by the *Rb*-related gene *p107*. We also show that acute loss of *Rb* in senescent cells leads to reversal of the cellular senescence programme. Thus, the use of conditional knockout strategies might refine our understanding of gene function and help to model human cancer more accurately.

To model somatic inactivation of *RB* in human cancer, we have created a conditional allele of the mouse *Rb* gene by using gene targeting in embryonic stem cells (Fig. 1a)[4]. Correct targeting and the presence of *lox*P sites flanking *Rb* exon 3 were verified by polymerase chain reaction (PCR) and Southern blot analysis (data not shown). Conditional *Rb* homozygous mutant mice displayed no developmental defects[5], and ageing mice did not develop tumours associated with the loss of *Rb* (J.S. and T.J., unpublished observations), indicating that this conditional allele was wild-type for *Rb* function before further deletion by the Cre recombinase. The proliferation rate of conditional *Rb* homozygous mouse embryonic fibroblasts ($cRb^{lox/lox}$ MEFs) was indistinguishable from that of wild-type MEFs, and the levels of pRB were identical in $cRb^{lox/lox}$ MEFs and in wild-type MEFs (data not shown).

When exponentially growing $cRb^{lox/lox}$ MEFs were infected with an adenovirus vector expressing the Cre recombinase (Ad-Cre), *Rb* exon 3 was deleted within 24 h (Fig. 1b). pRB was no longer detectable 3 days after infection with Ad-Cre (Fig. 1c). Levels of the two pRB family members p107 and p130 were not significantly affected by loss of pRB in exponentially growing populations, except

for a slight but reproducible increase in p107 levels (Fig. 1c). Levels of p107 are also elevated in germline $Rb^{-/-}$ MEFs[6]. We did not observe any inhibitory or growth-promoting effect of Ad or Ad-Cre infection on the proliferation of wild-type, $Rb^{-/-}$ and $cRb^{lox/lox}$ cells, indicating that, at the dose used, Ad-Cre is not cytotoxic in this system and that Ad or Ad-Cre does not cooperate with loss of pRB in cell cycle deregulation (Fig. 1d and data not shown). In addition, $Rb^{-/-}$ and $cRb^{-/-}$ MEFs had similar proliferation curves, showing that, in this respect, germline and acute loss of *Rb* function were phenotypically equivalent (Fig. 1e). $Rb^{-/-}$ and $cRb^{-/-}$ MEFs were indistinguishable in several other assays as well, including response to contact inhibition and proliferation at low density (data not shown). In summary, we have developed a system to eliminate *Rb* function acutely in primary MEFs. This system has allowed us to explore conditions under which acute *Rb* mutation might differ from the constitutive absence of *Rb*.

Maintenance of the growth-arrested state (quiescence) is crucial for normal development and differentiation. Failure to maintain quiescence can cause inappropriate proliferation, which can increase the target size for additional cancer-promoting mutations and can directly promote tumorigenesis. We therefore chose to study the consequences of acute loss of *Rb* function in quiescent cells. MEFs were first growth-arrested for 3 days at full confluence without the addition of fresh medium. The confluent cells were then rendered quiescent by leaving them for 3 days in 0.1% serum and for a further 3 days after replating in 0.1% serum at ~50% confluence. Quiescent germline $Rb^{-/-}$ MEFs were infected with Ad or Ad-Cre and kept for 3 days in 0.1% serum before incubation for 24 h with 5-bromodeoxyuridine (BrdU). Under these conditions, ~20% of the $Rb^{-/-}$ cells incorporated BrdU (Fig. 2a). For quiescent $cRb^{lox/lox}$ MEFs, either untreated or Ad-infected, ~10% of the cells incorporated BrdU in a 24-hour period (Fig. 2a). These data indicate that, as reported previously[7], germline loss of *Rb* function does not prevent cells from arresting in G0, but germline $Rb^{-/-}$ cells may be slightly resistant to G0 arrest induced by low serum concentration. Strikingly, however, quiescent $cRb^{lox/lox}$ MEFs infected with Ad-Cre showed a marked increase in the percentage of cells incorporating BrdU (~50% BrdU-positive cells in a 24-hour period; Fig. 2a), showing that acute loss of *Rb* is phenotypically different from its constitutive absence in this assay.

The relative normality of germline $Rb^{-/-}$ MEFs might be due to differences in the levels of cell cycle regulators compared with those in quiescent $cRb^{-/-}$ cells. The candidate cell cycle inhibitors $p21^{CIP1}$ and $p16^{INK4a}$ were expressed at similar levels in quiescent $cRb^{lox/lox}$ and $Rb^{-/-}$ MEFs (Fig. 2b). In contrast, targets of the E2F transcription factor, whose activity is deregulated in *Rb* mutant cells[8], were significantly upregulated in quiescent $Rb^{-/-}$ MEFs (Fig. 2b) compared with $cRb^{lox/lox}$ MEFs. However, some of these E2F target genes, such as *E2f-1* itself and the *cyclin E* gene, would be expected to promote cell cycle entry, and their upregulation cannot explain why germline *Rb* mutant cells were capable of entering and maintaining quiescence. The E2F target genes and cell cycle inhibitors $p19^{ARF}$ and *p107* were also markedly upregulated in quiescent $Rb^{-/-}$ MEFs compared with $cRb^{lox/lox}$ cells (Fig. 2b, c). Northern blot analysis (Fig. 2d) and real-time PCR (not shown) showed that p107 upregulation occurred largely at the transcriptional level, probably as a result of increased E2F activity in these cells. p130 protein levels were similar in the two populations (Fig. 2c).

To test the hypothesis that elevated levels of p107 in quiescent $Rb^{-/-}$ cells were at least partly responsible for their growth-arrested state, we sought to downregulate *p107* expression by the stable infection of exponentially dividing $Rb^{-/-}$ MEF populations with a retroviral vector allowing the production of small interfering RNA (siRNA) molecules directed against *p107* ('si-p107'). si-p107 $Rb^{-/-}$ MEFs expressed barely detectable levels of p107 but unchanged levels of p130 (Fig. 2e). The role of p107 in controlling the entry of $Rb^{-/-}$ MEFs in quiescence was first assayed by comparing proliferation indices in cells 24 h after the removal of growth factors (0.1% serum) with cells grown in 10% serum using incubation with BrdU for 1 h. At low serum concentration, the number of $Rb^{-/-}$ MEFs infected with a control retrovirus that incorporated BrdU decreased 2.9 ± 0.5-fold (mean ± s.d., $n = 7$) compared with cells

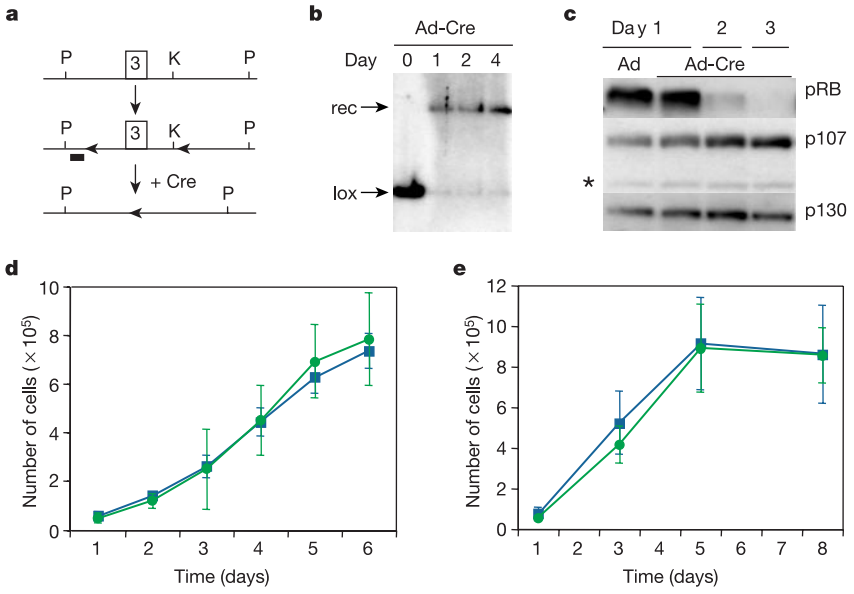

Figure 1 Acute deletion of *Rb* in MEFs. **a**, Creation of a conditional allele of *Rb*. After targeting, *Rb* exon 3 is flanked by *lox*P sites (arrow heads). After Cre-mediated recombination, *Rb* exon 3 is deleted, leaving one *lox*P site in the genome. P, *Pst*I, K, *Kpn*I. **b**, Southern blot analysis of *Rb* exon 3 deletion after infection of $cRb^{lox/lox}$ MEFs with Ad-Cre. lox, conditional allele; rec, recombined deleted allele. Genomic DNA was digested with *Pst*I and *Kpn*I. The probe used corresponds to the black box in **a**. **c**, Immunoblot analysis of the three pRB-family members after infection of proliferating $cRb^{lox/lox}$ MEFs with Ad or Ad-Cre (asterisk, non-specific protein band). **d**, Proliferation curve of $cRb^{lox/lox}$ MEFs infected with Ad (squares) or Ad-Cre (circles) ($n = 5$). **e**, Proliferation curve of $cRb^{lox/lox}$ ($cRb^{-/-}$, squares) and $Rb^{-/-}$ (circles) MEFs infected with Ad-Cre ($n = 6$).

grown at full serum concentration (~30% BrdU-positive cells for all the different populations studied). In contrast, the number of si-p107 $Rb^{-/-}$ cells incorporating BrdU decreased only 1.6 ± 0.4-fold (mean ± s.d., $n = 5$) in 0.1% serum compared with 10% serum, indicating that p107 plays a role in the entry of $Rb^{-/-}$ MEFs into quiescence.

We then attempted to make $Rb^{-/-}$ and si-p107 $Rb^{-/-}$ MEF populations fully quiescent after 6 days in 0.1% serum by following our initial protocol. The vast majority of quiescent si-p107 $Rb^{-/-}$ cells died under these conditions (not shown), a phenomenon similar to that previously observed with *Rb*-family triple knockout cells[4]. To bypass the death of si-p107 $Rb^{-/-}$ MEFs entering full quiescence, we used a lentiviral vector co-expressing a reporter gene encoding green fluorescent protein (GFP) and the same siRNA molecules directed against *p107* (ref. 9). In contrast to MLV-derived retroviruses, lentiviruses can infect non-dividing, quiescent cells. p107 knock-down in already quiescent lentivirus-infected $Rb^{-/-}$ MEFs was confirmed by western blot analysis and immunofluorescence (data not shown). Significantly, loss of p107 in quiescent $Rb^{-/-}$ MEFs led to a threefold increase in BrdU incorporation, showing that p107 expression is indeed necessary for the maintenance of quiescence in $Rb^{-/-}$ MEFs (Fig. 2f). Similar experiments with siRNA molecules directed against $p19^{ARF}$ indicated that $p19^{ARF}$ is also required for the establishment of full quiescence in $Rb^{-/-}$ MEFs (Supplementary Fig. 1).

The fact that levels of p107 are mostly controlled transcriptionally suggested that c$Rb^{-/-}$ cells might compensate rapidly for the loss of *Rb*. This possibility was also indicated by the fact that cycling early-passage $Rb^{-/-}$ and c$Rb^{-/-}$ MEFs had otherwise similar properties (see Fig. 1). In fact, we found that infection of c$Rb^{lox/lox}$ MEFs at the time when medium was changed to 0.1% serum (6 days before the time that we consider the cells to be quiescent) rendered them similar to $Rb^{-/-}$ MEFs with regard to p107 levels (data not shown) and BrdU incorporation (Fig. 2g). Thus, we conclude that transcriptional upregulation of *p107*, along with upregulation of $p19^{ARF}$ in quiescent germline $Rb^{-/-}$ cells can functionally compensate for loss of *Rb* and allows these cells to respond to anti-proliferative signals. In contrast, in cells in which pRB is actively involved in maintaining the quiescent state, such potential compensatory mechanisms are not deployed, allowing an acute loss of *Rb* to result in marked cell cycle re-entry.

We next examined whether other forms of cell cycle arrest were dependent on the continuous presence of pRB. It has been proposed that cellular senescence is an anti-cancer programme whose end-point is permanent cell cycle arrest, preventing ageing or mutant cells from undergoing proliferation[10–12]. $Rb^{-/-}$ MEFs undergo

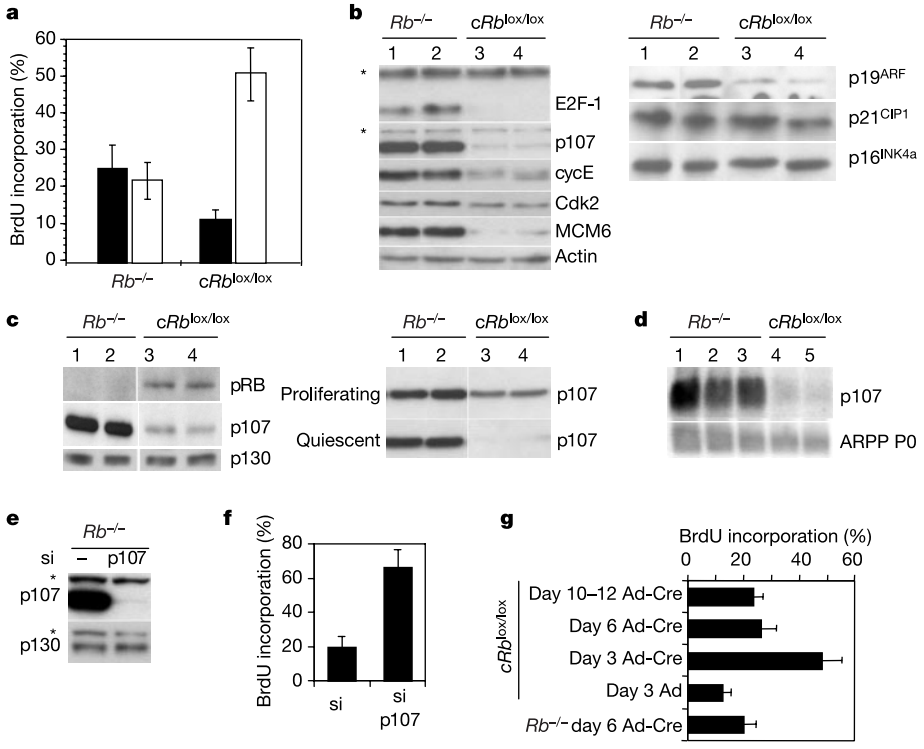

Figure 2 Effects of acute versus germline loss of *Rb* function in quiescent cells. **a**, Incorporation of BrdU into quiescent $Rb^{-/-}$ ($n = 4$) and c$Rb^{lox/lox}$ ($n = 6$) MEFs infected with Ad (filled bars) or Ad-Cre (open bars) and incubated with BrdU for 24 hours at 3 days after infection. Under the same conditions, more than 90% incorporation occurs in proliferating cells (not shown). **b**, Immunoblot analysis of E2F target genes and cell cycle inhibitors in two representative independent quiescent $Rb^{-/-}$ (lanes 1 and 2) and c$Rb^{lox/lox}$ (lanes 3 and 4) MEF populations before infection with Ad or Ad-Cre (asterisk, non-specific protein bands). **c**, Left, immunoblot analysis of pRB family members in quiescent $Rb^{-/-}$ (lanes 1 and 2) and c$Rb^{lox/lox}$ (lanes 3 and 4) MEF populations before infection with adenovirus. Right, comparison of p107 levels in proliferating and quiescent $Rb^{-/-}$ (lanes 1 and 2) and c$Rb^{lox/lox}$ (lanes 3 and 4) MEF populations before infection with adenovirus. Levels of p107 are lower in quiescent $Rb^{-/-}$ cells than in proliferating $Rb^{-/-}$ cells (not shown); different exposures were used to show the relative difference between the two conditions. A non-specific protein immunoreactive band confirmed equal loading (not shown). **d**, Northern blot analysis of *p107* RNA in quiescent $Rb^{-/-}$ (lanes 1–3) and c$Rb^{lox/lox}$ (lanes 4–6) MEF populations using a probe encompassing *p107* exon 8. Levels of the control *ARPP P0* RNA are similar in the two populations. **e**, Western blot analysis of p107 in $Rb^{-/-}$ MEFs stably infected with a control retrovirus (–) or a retrovirus producing siRNA molecules against *p107* (si-p107; 19-mer 5′-GATGTTGTCAGTGAGAGAG-3′) (asterisk, non-specific protein bands). **f**, Incorporation of BrdU into fully quiescent GFP-positive $Rb^{-/-}$ MEFs ($n = 3$) infected with a control GFP lentivirus (si) or a GFP lentivirus expressing siRNA molecules against *p107* (si-p107) and incubated with BrdU for 24 h at 3 days after infection. **g**, Time course of BrdU incorporation into quiescent c$Rb^{lox/lox}$ MEFs after infection with Ad-Cre. Cells were infected with Ad or Ad-Cre 3, 6 or 10–12 days before they were considered quiescent in our initial protocol.

senescence in culture[4,13,14]. However, MEFs with targeted deletion of all three *Rb* family members do not[4,13]. These data could indicate that the different members of the pRB family are equally capable of inducing and maintaining the senescent state, another example of functional overlap and functional compensation within this gene family. However, this compensation is difficult to reconcile with the fact that, whereas *RB* mutations are common in human cancer, *p107* and *p130* mutations occur rarely, if ever[15].

We therefore decided to study the effect of acute *Rb* mutation in senescent cells. We found that p107 concentrations were higher in senescent $Rb^{-/-}$ MEFs than in senescent wild-type MEFs (Fig. 3a), indicating that p107 might also compensate for a loss of pRB in this system. $cRb^{lox/lox}$ MEFs were cultured following 3T3 or a 3T2 protocol[16]; they were infected with Ad or Ad-Cre when they reached senescence and stopped accumulating (passage 8–12 of a 3T2 assay). Because populations of senescent cells are not fully synchronized and can contain a subpopulation of immortalized clones, we excluded cultures in which more than 15% of cells were BrdU-positive. The selected $cRb^{lox/lox}$ MEF populations were infected with Ad or Ad-Cre, and 3 days later (to allow pre-existing pRB protein to be degraded; see Fig. 1c), BrdU was added for 24 h before fixation and staining. Under these conditions, senescent Ad-infected cells displayed 10–20% BrdU-positive cells. In contrast, after infection with Ad-Cre, 50% of these cells became BrdU-positive (Fig. 3b), indicating that the cell cycle arrest associated with senescence can be reversed after acute loss of *Rb*. This result was confirmed in early-passage $cRb^{lox/lox}$ MEFs induced to senesce prematurely with a retroviral construct expressing high levels of oncogenic Ras ($H\text{-}Ras^{V12}$)[17] (Fig. 3c).

Human senescent cells remain blocked in G2 or die after induction of the simian virus 40 large T oncoprotein[18]. In contrast, 27 of 100 senescent $cRb^{lox/lox}$ cells infected with Ad-Cre rounded up 3 days after addition of virus (and only 2 of 100 in Ad-infected cells), as observed with a recording period of 40 h using time-lapse videomicroscopy (Supplementary Fig. 2). These experiments confirm that senescent $cRb^{lox/lox}$ cells can complete the cell cycle after an acute loss of *Rb* function.

Injection of anti-p53 antibodies has been shown to reverse the senescent state in human cells temporarily[19]. To determine whether dividing post-senescent $cRb^{-/-}$ MEF populations could undergo multiple cell divisions, $cRb^{lox/lox}$ cells were subjected to the 3T3 protocol until they reached senescence (as assessed by morphological changes and a lack of accumulation in cell number). Populations containing obvious small immortalized cells were not included for study. Selected senescent populations were then divided in two and infected with Ad or Ad-Cre. Ad-infected $cRb^{lox/lox}$ cells remained senescent and did not show an increase in cell number. In contrast, 14 of 16 $cRb^{lox/lox}$ MEF populations infected with Ad-Cre resumed

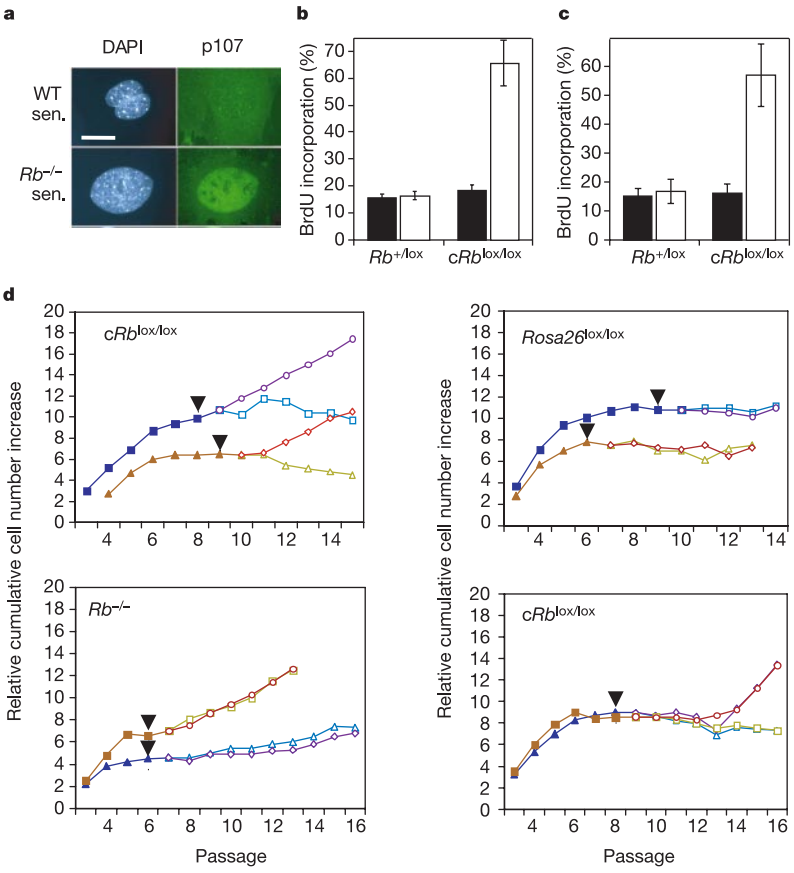

Figure 3 Reversal of senescence after acute loss of *Rb*. **a**, Immunostaining analysis of p107 levels (green) in wild-type (WT) and $Rb^{-/-}$ senescent (sen.) MEFs. Staining of the DNA with DAPI (blue) shows the nucleus. The specificity of the antibody was confirmed by the absence of nuclear signal from $p107^{-/-}$ MEFs (not shown). Scale bar, 50 μm. **b**, **c**, Senescent populations of $cRb^{lox/lox}$ ($n = 6$) and $cRb^{+/lox}$ ($n = 2$) MEFs obtained at the end of a 3T2 protocol (**b**) and prematurely senescent populations of $cRb^{lox/lox}$ ($n = 4$) and $cRb^{+/lox}$ ($n = 3$) MEFs expressing high concentrations of oncogenic $H\text{-}Ras^{V12}$ (**c**) were infected with Ad (filled bars) or Ad-Cre (open bars). After 3 days, BrdU was added for 24 h before fixation, staining and counting. **d**, $cRb^{lox/lox}$ (top left and bottom right panels), $Rb^{-/-}$ (bottom left) and $Rosa26^{lox/lox}$ (top right) MEFs were grown following a 3T3 protocol (two representative examples are shown, filled squares and filled triangles). At senescence (arrow), MEFs were infected with Ad (top panels and bottom left) or LV-lacZ (bottom right, open squares and open triangles), or Ad-Cre (top panels and bottom left) or LV-Cre (bottom right, open circles and open diamonds).

proliferation and showed clear cell accumulation within three or four passages (Fig. 3d). PCR and immunoblot analysis showed that these growing cells had deleted *Rb* exon 3 and did not express pRB (data not shown). As controls for this experiment, we have shown that wild-type MEFs with *lox*P sites in a non-relevant gene (*Rosa26*; $n = 3$) and germline $Rb^{-/-}$ MEFs ($n = 3$) did not proliferate further after adenovirus infection (Fig. 3d). In addition, senescent $cRb^{lox/lox}$ cells infected with a lentiviral vector expressing *Cre* (LV-Cre)[20] re-entered the cell cycle and resumed proliferation ($n = 3$), whereas cells infected with a control virus (LV-lacZ) remained senescent (Fig. 3d). The slower accumulation of cells after infection with LV-Cre might be due to the fact that only ~50–60% of the cells were infected by the lentiviral vector as assessed by β-galactosidase staining. Finally, post-senescent cycling $cRb^{-/-}$ cells remained sensitive to the reintroduction of *Rb* (data not shown), indicating that cells had not undergone major mutations after the reversal of senescence.

Further analysis of post-senescent $cRb^{-/-}$ cells showed that other markers associated with senescence (cell size, plasminogen activator inhibitor-1 (PAI-1)) were also dependent on *Rb* function, indicating that pRB might control multiple downstream aspects of the senescence programme (Supplementary Fig. 3). The p53 pathway was still intact, and levels of $p19^{ARF}$, $p16^{INK4a}$ and $p21^{CIP1}$ also remained constant or increased in cycling post-senescent $cRb^{-/-}$ cells in comparison with pre-senescent and senescent cells (Supplementary Fig. 3). Levels of p107 also increased in senescent $cRb^{lox/lox}$ cells 4 days after the loss of *Rb* and in further passages (data not shown). It is difficult to know whether the increase in $p19^{ARF}$ and p107 levels occurred because more cells were in active cycle or whether it was a direct result of a compensatory mechanism. One might expect that increased levels in cell cycle inhibitors in post-senescent $cRb^{-/-}$ cells would ultimately lead to the re-establishment of senescence, even though cycling cells in 10% serum might be less sensitive than quiescent or senescent cells to their growth-inhibitory action. Indeed, 2 of 14 $cRb^{-/-}$ MEF populations re-entered senescence at passage 18–20 (data not shown). The long-term fate of the remaining populations was uncertain owing to the emergence of immortalized clones. The results of these experiments strongly suggest that senescent MEFs can re-enter the cell cycle, divide and proliferate after the acute loss of *Rb*, even in cells with wild-type *p107* and *p130*. Similar results have recently been obtained after loss of *p53* function in MEFs[21]; taken together, these results show that the senescence-induced cell cycle arrest is not an irreversible process.

By studying two cellular contexts, quiescence and senescence, we describe functions for the *Rb* tumour suppressor gene that were not apparent from previous analysis with cells derived from germline $Rb^{-/-}$ embryos. These results have important implications for the interpretation of knockout studies generally, and they might also inform the design of mouse models of cancer involving *RB* and other cancer-associated genes. The most likely explanation for the relative normality of $Rb^{-/-}$ cells in culture is functional compensation by the family members p107 and p130. Thus, $Rb^{-/-}$ cells might upregulate p107 to help establish and maintain quiescent and senescent cell cycle arrest. However, in a situation of functional overlap and potential functional compensation, it is difficult to explain why the loss of a given gene function (for example, *Rb*) during tumorigenesis would have a significant effect. Our data might help to resolve this apparent conflict. By detecting phenotypic differences between conditional and acute loss of *Rb* function, we conclude that functional compensation is context dependent. Although such compensation clearly can occur, it might require a more prolonged absence of *Rb* function and a more complex resetting of the cell cycle machinery. Therefore, simple, acute loss of *Rb* can by itself stimulate quiescent and senescent cells to re-enter the cell cycle. The additional rounds of cell division that would ensue from an acute loss of *Rb* function could be crucial in the control of tumour initiation and progression. Given these considerations, cancer modelling strategies that employ a conditional loss of *Rb*[22,23], other tumour suppressor genes and even gain-of-function mutations[2,3] might be important in accurately recapitulating the effects of spontaneous mutations in human cancer. □

Methods

Embryonic stem cells and gene targeting

Two embryonic stem cell clones were introduced into the germline of mice, one in which the puromycin selection cassette was left in the intron downstream of exon 3 (ref. 4), and another in which this cassette was excised after the transient expression of Cre in embryonic stem cells. Cells produced from mice derived from the two types of clones gave identical results.

Culture of MEFs

All experiments were performed with MEFs prepared from embryos from at least two different litters in a mixed 129Sv/J:C57Bl/6 background. MEFs with *lox*P sites flanking a transcriptional stop cassette upstream of the *lacZ* gene in the *Rosa26* locus ($Rosa26^{lox/lox}$) were generated from mice provided by Dr S. Orkin. Serial 3T2 and 3T3 cultivation was conducted as described[4,16].

MEFs were infected with high-titre retroviral or lentiviral stocks produced by the transient transfection of 293T cells[4,9]. After infection with the pSIRIPP retrovirus allowing the expression of siRNA molecules (a derivative of pSuper[24] and pQCXN, provided by S. Lessnick), MEFs were selected with 2 μg ml^{-1} puromycin. After infection with the pWZL-H-Ras^{V12} retrovirus (a gift from D. Tuveson), MEFs were selected with 75 μg ml^{-1} hygromycin B.

Adenoviral stocks were purchased from the Gene Transfer Vector Core facility of University of Iowa College of Medicine. About 100 plaque-forming units of virus were used per cell, and the medium was changed 1 day after infection.

Cell cycle, cell size and cell death assays

These assays were performed as described[4]. DNA synthesis was assayed by the incorporation of BrdU (3 μg ml^{-1}; Sigma) for 24 h with an anti-BrdU antibody coupled with fluorescein isothiocyanate (Roche; dilution 1:50) or a rat anti-BrdU antibody (Becton Dickinson; dilution 1:500). At least 500 cells were counted for each experiment.

Immunodetection

Western blot analysis of whole-cell extracts for cell cycle proteins and PAI-1 (Transduction Laboratories, P30620; dilution 1:1000) was performed as described[4]. Immunofluorescence analysis of p107 was performed on paraformaldehyde-fixed cells by using the SD15 monoclonal antibody (Neomarkers; dilution 1:20).

RNA analysis

RNA preparation and northern blot analysis were performed as described[4]. *p107* and *p130* oligonucleotides designed for real-time PCR span several exons at the 3′ end of the complementary DNAs; sequences and protocol are available upon request.

Received 19 March; accepted 1 May 2003; doi:10.1038/nature01764.

1. Hanahan, D. & Weinberg, R. A. The hallmarks of cancer. *Cell* **100,** 57–70 (2000).
2. Van Dyke, T. & Jacks, T. Cancer modelling in the modern era: Progress and challenges. *Cell* **108,** 135–144 (2002).
3. Jonkers, J. & Berns, A. Conditional mouse models of sporadic cancer. *Nature Rev. Cancer* **2,** 251–265 (2002).
4. Sage, J. *et al.* Targeted disruption of the three Rb-related genes leads to loss of G_1 control and immortalization. *Genes Dev.* **14,** 3037–3050 (2000).
5. MacPherson, D. *et al.* Conditional mutation of Rb causes cell cycle defects without apoptosis in the central nervous system. *Mol. Cell. Biol.* **23,** 1044–1053 (2003).
6. Hurford, R. K. Jr, Cobrinik, D., Lee, M. H. & Dyson, N. pRB and p107/p130 are required for the regulated expression of different sets of E2F responsive genes. *Genes Dev.* **11,** 1447–1463 (1997).
7. Lomazzi, M., Moroni, M. C., Jensen, M. R., Frittoli, E. & Helin, K. Suppression of the p53- or pRB-mediated G1 checkpoint is required for E2F-induced S-phase entry. *Nature Genet.* **31,** 190–194 (2002).
8. Trimarchi, J. M. & Lees, J. A. Sibling rivalry in the E2F family. *Nature Rev. Mol. Cell Biol.* **3,** 11–20 (2002).
9. Rubinson, D. A. *et al.* A lentivirus-based system to functionally silence genes in primary mammalian cells, stem cells and transgenic mice by RNA interference. *Nature Genet.* **33,** 401–406 (2003).
10. Hayflick, L. & Moorhead, P. S. The serial cultivation of human diploid cell strains. *Exp. Cell Res.* **25,** 585–621 (1961).
11. Campisi, J. Cellular senescence as a tumour-suppressor mechanism. *Trends Cell Biol.* **11,** S27–S31 (2001).
12. Schmitt, C. A. *et al.* A senescence program controlled by p53 and $p16^{INK4a}$ contributes to the outcome of cancer therapy. *Cell* **109,** 335–346 (2002).
13. Dannenberg, J. H., van Rossum, A., Schuijff, L. & te Riele, H. Ablation of the retinoblastoma gene family deregulates G_1 control causing immortalization and increased cell turnover under growth-restricting conditions. *Genes Dev.* **14,** 3051–3064 (2000).
14. Carneiro, C. *et al.* p27 deficiency desensitizes $Rb^{-/-}$ cells to signals that trigger apoptosis during pituitary tumour development. *Oncogene* **22,** 361–369 (2003).
15. Classon, M. & Harlow, E. The retinoblastoma tumour suppressor in development and cancer. *Nature Rev. Cancer* **2,** 910–917 (2002).
16. Todaro, G. & Green, H. Quantitative studies of the growth of mouse embryo cells in culture and their development into established lines. *J. Cell Biol.* **17,** 299–313 (1963).
17. Serrano, M., Lin, A. W., McCurrach, M. E., Beach, D. & Lowe, S. W. Oncogenic ras provokes premature

cell senescence associated with accumulation of p53 and p16INK4a. *Cell* **88,** 593–602 (1997).
18. Jat, P. S. & Sharp, P. A. Cell lines established by a temperature-sensitive simian virus 40 large-T-antigen gene are growth restricted at the nonpermissive temperature. *Mol. Cell. Biol.* **9,** 1672–1681 (1989).
19. Gire, V. & Wynford-Thomas, D. Reinitiation of DNA synthesis and cell division in senescent human fibroblasts by microinjection of anti-p53 antibodies. *Mol. Cell. Biol.* **18,** 1611–1621 (1998).
20. Pfeifer, A., Brandon, E. P., Kootstra, N., Gage, F. H. & Verma, I. M. Delivery of the Cre recombinase by a self-deleting lentiviral vector: Efficient gene targeting *in vivo*. *Proc. Natl Acad. Sci. USA* **98,** 11450–11455 (2001).
21. Dirac, A. M. & Bernards, R. Reversal of senescence in mouse fibroblasts through lentiviral suppression of p53. *J. Biol. Chem.* **278,** 11731–11734 (2003).
22. Vooijs, M., van der Valk, M., te Riele, H. & Berns, A. Flp-mediated tissue-specific inactivation of the retinoblastoma tumour suppressor gene in the mouse. *Oncogene* **17,** 1–12 (1998).
23. Marino, S., Vooijs, M., van Der Gulden, H., Jonkers, J. & Berns, A. Induction of medulloblastomas in p53-null mutant mice by somatic inactivation of Rb in the external granular layer cells of the cerebellum. *Genes Dev.* **14,** 994–1004 (2000).
24. Brummelkamp, T. R., Bernards, R. & Agami, R. A system for stable expression of short interfering RNAs in mammalian cells. *Science* **296,** 550–553 (2002).

Supplementary Information accompanies the paper on **www.nature.com/nature**.

Acknowledgements We thank R. Jaenisch, S. Lowe and B. Kennedy for various useful reagents; D. Tuveson for helpful discussions; A. Brunet, K. Johnson and M. McLaughlin for critical reading of the manuscript; and members of F. Gertler's laboratory for help with the videomicroscopy experiments. This work was supported by funding from the Human Frontier Science Program, the Medical Foundation and the Merck/MIT postdoctoral fellowship program (J.S.), and from the National Cancer Institute and the Howard Hughes Medical Institute (T.J.).

Competing interests statement The authors declare that they have no competing financial interests.

Correspondence and requests for materials should be addressed to T.J. (tjacks@mit.edu).

Xpd/Ercc2 regulates CAK activity and mitotic progression

Jian Chen, Stéphane Larochelle*, Xiaoming Li & Beat Suter

Department of Biology, McGill University, Montreal, PQ, Canada H3A 1B1

General transcription factor IIH (TFIIH) consists of nine subunits: cyclin-dependent kinase 7 (Cdk7), cyclin H and MAT1 (forming the Cdk-activating-kinase or CAK complex), the two helicases Xpb/Hay and Xpd, and p34, p44, p52 and p62 (refs 1–3). As the kinase subunit of TFIIH, Cdk7 participates in basal transcription by phosphorylating the carboxy-terminal domain of the largest subunit of RNA polymerase II[1,4,5]. As part of CAK, Cdk7 also phosphorylates other Cdks, an essential step for their activation[6–9]. Here we show that the *Drosophila* TFIIH component Xpd negatively regulates the cell cycle function of Cdk7, the CAK activity. Excess Xpd titrates CAK activity, resulting in decreased Cdk T-loop phosphorylation, mitotic defects and lethality, whereas a decrease in Xpd results in increased CAK activity and cell proliferation. Moreover, Xpd is downregulated at the beginning of mitosis when Cdk1, a cell cycle target of Cdk7, is most active. Downregulation of Xpd thus seems to contribute to the upregulation of mitotic CAK activity and to regulate mitotic progression positively. Simultaneously, the downregulation of Xpd might be a major mechanism of mitotic silencing of basal transcription.

With its dual role, Cdk7 might function as a critical link between the cell cycle and transcriptional programmes[1,6,10]. To identify genes involved in directing Cdk7 activity towards transcription or cell-cycle function in a multicellular organism, we screened for dominant suppressors and enhancers of a hypomorphic *Drosophila* $cdk7^{ts1}$ mutant that has a cell cycle but no transcriptional defect. We found that decreasing *xpd/Ercc2* (xeroderma pigmentosum disorder group D/excision repair cross-complementing) strongly suppresses the hypomorphic $cdk7^{ts1}$ cell-cycle defect (Supplementary Information).

The first 13 mitotic cycles of the *Drosophila* embryo are synchronized syncytial cycles that do not require transcription and are composed of only the S and M phases. During cycle 14, cell divisions become asynchronous[11] and zygotic transcription increases strongly. On such embryos the anti-Xpd antibody produces a highly cell-cycle-dependent staining pattern (Fig. 1a–e). Figure 1a–c shows asynchronic cells of a wild-type embryo at cycle 14. In interphase and prophase cells, a strong Xpd signal is found. In cells at metaphase, anaphase and telophase, the signal drops to almost background levels. A similar pattern was observed in embryos at cycle 15 (not shown), and in embryos at cycle 13 the Xpd signal is significantly lower during metaphase than in interphase (Fig. 1d, e). In contrast, immunostaining with antibodies against Xpb/Hay did not show this cell-cycle dependence (not shown).

To find out whether the drop in Xpd signal is caused by the downregulation of Xpd, Schneider cells were synchronized at G2/M and aliquots of the cells were collected at the indicated time points after release from the block (Fig. 1f). Starting at 120 min, the percentage of cells in G1 increases at the expense of G2/M cells, indicating that G2/M arrested cells have started to progress through mitosis. Also at 120 min the Xpd concentrations start to drop. At 240 min, Xpd has reached its lowest concentration, coinciding with the rapid downregulation of cyclin B and cyclin A. Together with the embryonic *in situ* staining data, this result indicates that the Xpd polypeptide is downregulated during prometaphase.

To test whether low Xpd concentrations are required for normal CAK activity and for cells to go through mitosis, we overexpressed Xpd in 2–4-h-old embryos. Embryos containing two copies of the *hsp–xpd* transgene were heat shocked for 30 min at 36 °C, and CAK activity was measured after recovery. Extracts from transgenic embryos had significantly less CAK activity than non-transgenic controls (Fig. 2a, b). To find out whether these differences in CAK activity are physiologically relevant, Cdk1 phosphorylation was analysed after pulse induction of Xpd. *Drosophila* Cdk1 polypeptide can be resolved into three to four isoforms, with the fastest migrating isoform, isoform 1, being the Thr 161-phosphorylated Cdk1 (Fig. 2c)[12]. In a comparable manner to non-heat-shocked wild-type flies, wild-type embryos have significant concentrations of the Thr 161-phosphorylated isoform 1 after a 60-min recovery period. However, in flies containing the *hsp–xpd* transgene, the Thr 161-phosphorylated isoform is still undetectable after 60 min of recovery. Overexpression of Xpd thus results in less phosphorylation of Cdk1 on Thr 161.

In 2–3-h-old wild-type embryos, the heat treatment caused only 10% of the embryos to show a lethal phenotype 90 min into the recovery period. However, on overexpression of *xpd*, 50% of the embryos showed lethality (Fig. 2d) as judged by large areas of DNA aggregation, irregular mitotic figures and degenerating cells (not shown). The embryonic lethality is comparable to the overall lethality during the entire life, indicating that pulse overexpression of *xpd* in the embryo has a rapid effect only on embryonic viability and no long-term effects are caused by, for instance, general transcriptional problems. This lethality was not observed with control transgenic lines containing either *hsp–xpb/hay* or an *hsp–xpd* construct that lacks the amino-terminal CAK-interaction domain[13] (*hsp–xpdC*), indicating that decreased fly viability is indeed caused by greater Xpd concentrations (Fig. 2d).

We also tested the effect of different *xpd* dosage during the entire life cycle by using a co-culture assay with offspring from a single cross (Fig. 2e). After daily induction of *hsp–xpd* in addition to the wild-type *xpd* concentration, the viability of transgenic *hsp–xpd* lines (*CyO*/+; +/*hsp–xpd*) is decreased to 14% (36 of 251) compared with the wild-type 100% (*CyO*/+; +/*PrDr*). This decreased

* Present address: Cell Biology Program, Memorial Sloan-Kettering Cancer Center, New York, New York 10021, USA.

